# Ground-based temperature and humidity profiling using spectral infrared and microwave observations: Part 1. Retrieval performance in clear sky conditions

Ulrich Löhnert*, D.D. Turner**, S. Crewell*

*Institute for Meteorology and Geophysics, University of Cologne, GER

** Space Science and Engineering Center, University of Wisconsin-Madison, Madison, USA

Manuscript version June 17, 2008

submission to *Journal of Applied Meteorology and Climatology*

*Corresponding Author Address:*

*Dr. Ulrich Löhnert*

*Institute for Meteorology and Geophysics*

*Zülpicher Straße 49a*

*50674 Köln*

*Germany*

*Tel: +49 +221 470 1779*

*Fax: +49 +221 470 5161*

*Email: loehnert@meteo.uni-koeln.de*

**Abstract**

Two independent ground-based passive remote sensing methods are applied to retrieve lower tropospheric temperature and humidity profiles in clear-sky cases. A simulation study for two distinctly different climatic zones is performed to evaluate the accuracies of a standard microwave profiler (HATPRO) and an infrared spectrometer (AERI) by applying a unified optimal estimation scheme to each instrument. Different measurement modes for each instrument are also evaluated, where the retrieval uses different spectral channels and observational view angles. Additionally, both instruments have been combined into the same physically consistent retrieval scheme to evaluate the differences between a combined retrieval relative to the single-instrument retrievals. Generally the infrared measurements "outperform" the microwave measurements in both RMSE and bias error. The AERI retrievals show high potential, especially for retrieving humidity in the boundary layer, where accuracies are on the order of 0.25 - 0.5 g $m^{-3}$ for a central European climate. In the lowest 500 m the retrieval accuracies for temperature from elevation scanning microwave measurements and spectral infrared measurements are very similar (0.2 – 0.6 K). Above this level the accuracies of the AERI retrieval are significantly more accurate (< 1 km RMSE below 4 km). The inclusion of microwave measurements to the spectral infrared measurements within a unified physical retrieval scheme only results in improvements in the high-humidity tropical climate. However, compared to the HATPRO retrieval, the accuracy of the AERI retrieval is more sensitive to changes in the measurement uncertainty. The combined AERI-HATPRO retrieval algorithm is expected to yield beneficial results when clouds are included.

## 1. Introduction

High temporal resolution vertical profiles of atmospheric temperature and humidity are needed by many applications in atmospheric sciences, such as initialization of weather forecasting, model evaluation and process studies. Atmospheric stability is in particular described by the basic meteorological quantities, namely temperature and humidity profiles. Even today, radiosondes continue to provide a benchmark measurement for determining high-resolution vertical profiles of pressure, temperature, humidity and wind because all of the parameters can be simultaneously determined and the accuracy is acceptable for a number of meteorological and aerological applications. Operational radiosonde soundings, however, typically provide 12-hourly observations; a temporal resolution which is often not sufficient for many meteorological applications, such as boundary layer (BL) transitions or frontal passages. Also a radiosonde ascent drifts with the wind, which can lead to a significant horizontal displacement and the ascent as such will take ~1h to profile the troposphere; both of these factors leading to a sampling error. Additionally many radiosonde sensors show a "dry bias" behavior during the day time (e.g. Cady-Pereira et al. 2008; Turner et al. 2003) – an error which is difficult to account for due to its dependence on multiple environmental factors.

Different remote sensing methods have the advantage of being able to derive profile information of temperature and humidity with a high temporal resolution, but suffer some drawbacks in vertical resolution and accuracy. This paper compares the performance of ground-based temperature and humidity profiling methods in two different spectral regions: microwave and infrared. Using identical retrieval approaches we will address the following questions: **What are the respective merits of microwave and infrared ground-based temperature and humidity profiling and what can be gained from a combination of both?** This study (Part 1) focuses on purely clear sky conditions and the goal is to analyze retrieval performance in detail in order to pursue simultaneous temperature, humidity and cloud microphysical parameter retrieval in near future (Parts to follow, in preparation).

Passive **microwave radiometry** uses frequency bands around the water vapor absorption line at 22.235 GHz for water vapor profiling and around the 60 GHz oxygen complex for temperature profiling. Studies have shown that approximately 4-5 independent levels of temperature information may be obtained, whereas the number of independent water vapor levels is on the order of two (Löhnert et al. 2008, Hewison 2007). If elevation scanning measurements are additionally considered, temperature accuracies are within 0.5 K close to the ground and degrade with height to ~1-2 K in the lower troposphere, whereas humidity accuracies range on the order of ~0.8 $gm^{-3}$. These values are more or less independent on the occurrence of clouds, expect for cases of heavy precipitation where saturation effects may occur or the instrument is influenced by rain water on the radome.

Previous studies have shown that multi-spectral measurements in the **infrared** contain information on the tropospheric temperature and humidity profile (Smith et al. 1999, Feltz et al. 2003). This information is generally limited to clear sky cases and cases where clouds are optically thin. However in case of optically thick cloud, information of temperature and humidity may still be obtained below the cloud if the cloud emissivity and temperature are known or retrieved.

In the following, we describe the parallel development of microwave (MW) and infrared (IR) techniques for temperature and humidity retrieval for clear sky cases using the same optimal estimation retrieval framework for each. These retrieval algorithms are applied to a typical central European climate and a humid tropical climate in order to be able to interpret the results as a function of vertically integrated water vapor amount (IWV).

Our goal is to analyze the error characteristics of both approaches and additionally, to combine both measurements into one scheme to evaluate the accuracy that is obtained in a joint retrieval algorithm. The results shown in this study are purely based on virtual measurements derived from radiative transfer simulations to be able to carry out a "clean" error analysis. In this way we can exclude sources of bias error due to erroneous calibration and absorption model uncertainties – errors which are difficult to quantify in general.

The characteristics of the microwave and infrared instruments used for simulation are described in section 2 of this paper, whereas the retrieval framework, which consists of an optimal estimation approach, is described in section 3. In section 4 we evaluate the accuracies of the retrieval procedures, whereby the MW and IR techniques are separately applied to the same cases and compared to each other. We examine the benefits of combining MW and IR approaches in one joint retrieval and also evaluate the impact of using different IR bands and microwave measurement approaches (zenith-only observations vs. zenith plus elevation scanning observations). Finally in section 6 we provide a summary and an outlook towards describing the cloudy atmosphere with the expected powerful combination MW plus IR.

## 2. Instrumentation

In the following the principles of the microwave profiler HATPRO (Humidity And Temperature PROFiler) and the infrared interferometer AERI (Atmospheric Emittance Radiance Interferometer) are briefly described.

### 2.1. HATPRO

The microwave profiler HATPRO was designed as a network-suitable low-cost microwave radiometer which can observe liquid water path (LWP), humidity and temperature profiles with high temporal resolution up to 1s (Rose et al. 2005). HATPRO consists of total-power radiometers utilizing direct detection receivers within two bands M1 and M2 (see Tab. 1, Fig. 1). The channels of Band M1 contain information about the vertical profile of humidity through the pressure broadening of the optically thin 22.235 GHz $H_2O$ line, and also contain information on determining liquid water path (LWP). The channels of Band M2 contain information on the vertical profile of temperature due to the homogeneous mixing of $O_2$ throughout the atmosphere. At the opaque center of the $O_2$ absorption complex at 60 GHz, most of the information originates from near the surface, whereas further away from the line, the atmosphere becomes less and less opaque so that more and more information also originates from higher atmospheric layers.

In addition to the spectral information, angular information can enhance the accuracy of the temperature profile in the boundary layer (Crewell and Löhnert 2007) when the atmosphere in the direct horizontal vicinity (~3km) of the microwave profiler is assumed to be horizontally homogeneous. Only the observations from the optically thick frequency bands close to 60 GHz are used in these elevation scans. Since the brightness temperatures vary only slightly with elevation angle, the method requires a highly sensitive radiometer (i.e., low random noise levels), which is typically realized by using wide bandwidths (up to 4 GHz) in these channels.

**2.2. AERI**

The AERI is a hardened, operational infrared spectrometer that measures the down-welling infrared radiance from 3.3-19 μm (3000 to 520 $cm^{-1}$, see Fig. 1) at 1 $cm^{-1}$ resolution (Knuteson et al. 2004a, b). Two detectors are used in a ‘sandwich’ configuration to provide the needed sensitivity across the entire spectral range. Details on the calibration approach and accuracy, as well as how the noise level in the AERI observations is determined, are provided by Knuteson et al. (2004 b). The AERI is typically run in one of two temporal sampling modes: (1) ‘normal-sample’ mode, whereby sky radiance is averaged for 3 minutes followed by views of the two calibration blackbodies, resulting in an approximate 7-min temporal resolution; and (2) ‘rapid-sample’ mode, where sky radiance is averaged for 12 s and multiple (8 to 10) sky averages are collected before the blackbodies are viewed. While the rapid-sample data has approximately 4 times more random noise than the normal-sample data, a principal component based noise filter is used to remove the uncorrelated random error from the AERI observations thereby resulting in a similar noise level in the rapid-sample data as that in the normal-sample data (Turner et al. 2006).

Like the microwave spectrum, the infrared spectrum also contains information on the vertical profile of temperature and humidity. Smith et al (1999) and Feltz et al (1998) used spectral observations from 612-713 $cm^{-1}$ and 2223-2260 $cm^{-1}$ (i.e., measurements from the 15 µm and 4.3 µm $CO_2$ bands, respectively) for temperature profiling, and observations from 538-588 $cm^{-1}$ and 1250-1350 $cm^{-1}$ (i.e., measurements from the wings of the rotational and 6.3 µm water vapor bands, respectively) for water vapor profiling. Our analysis demonstrated that the information content on both the longwave side (612-660 $cm^{-1}$) and shortwave side (675-713 $cm^{-1}$) of the 15 µm $CO_2$ band are essentially equivalent, and thus we will not include the observations from the 612-660 $cm^{-1}$ band in this study. Thus, our analysis focuses on the four distinct Bands A1-A4 of the AERI shown in Tab. 1.

## 3. Retrieval Methodology

The true atmospheric state vector $\mathbf{x}$, which we are retrieving in this study, consists of vertical profiles of atmospheric temperature ($\mathbf{T}$) and absolute humidity ($\boldsymbol{\rho}_v$), such that we can notate $\mathbf{x}=(\mathbf{T}, \boldsymbol{\rho}_v)$. [From here on vectors will be noted in bold (here i.e. profile vectors).] The vertical resolution used in the retrieval algorithm for both temperature and humidity is set to 50 m in the lowest 200 m and then increases gradually to 150 m at 1000 m, 250 m at 3000 m and 500 m at 10 km above the surface, which corresponds approximately to typical height grids used in state-of-the-art NWP models.

### 3.1. Measurement Inversion

The goal of the integrated profiling technique (IPT) algorithm is to retrieve $\mathbf{x}$ by optimally exploiting the information from a given measurement vector $\mathbf{y}$ (Rodgers, 2000). Depending on the situation, **y** will consist of a vector of observed microwave brightness temperatures and/or infrared radiances. Generally in remote sensing applications, determining **x** from **y** directly is an underdetermined and ill-conditioned problem, meaning that no unique solution exists and that very small errors in the measurement may lead to huge deviations in the retrieved atmospheric profile. Approaches to increase the number of degrees of freedom of the solution vector are to combine complementary measurements or add a source of *a priori information* to the retrieval problem, which is in our case the seasonal mean profile. If the relationship between **x** and **y** is slightly to moderately non-linear, an optimal atmospheric state $\mathbf{x}_{op}$ can be found by iterating the following formulation

$$\mathbf{x}_{i+1} = \mathbf{x}_i + \left(\mathbf{K}_i^T \mathbf{S}_e^{-1} \mathbf{K}_i + \mathbf{S}_a^{-1}\right)^{-1} \left[\mathbf{K}_i^T \mathbf{S}_e^{-1}\left(\mathbf{y} - \mathbf{y}_i\right) + \mathbf{S}_a^{-1}\left(\mathbf{x}_a - \mathbf{x}_i\right)\right] \quad (1)$$

where $i$ represents the iteration step, $\mathbf{x}_a$ the a priori knowledge of **T** and $\boldsymbol{\rho}_v$, $\mathbf{S}_a$ the a priori covariance matrix, and $\mathbf{S}_e$ the combined measurement and forward model error covariance matrix. $\mathbf{K}_i = \partial \mathbf{F}(\mathbf{x}_i)/\partial \mathbf{x}_i = \partial \mathbf{y}_i / \partial \mathbf{x}_i$ denotes the Jacobian, or the sensitivity of the forward model to changes in **x**, where $\mathbf{K}_i$ is re-calculated for each iteration. The forward model **F** transforms from the state space (**x**) to the measurement space (**y**) in a straight-forward way; i.e., given a state space vector at a certain iteration $\mathbf{x}_i$, **F** calculates $\mathbf{y}_i$ by applying a radiative transfer operator to compute the brightness temperatures and/or radiance at the microwave frequencies and/or the infrared wavenumbers. In the microwave case the radiative transfer operator consists of a 1D purely emission-based forward integration of the radiative transfer equation with a fast absorption predictor (Löhnert et al. 2004) based on the Rosenkranz 1998 millimeter-wave absorption model (Rosenkranz 1998) to enhance the speed of the Jacobian calculations. In the infrared case, the forward model is a fast transmittance model based upon Eyre and Woolf (1988). This 'fastaeri' model treats water vapor and ozone as variable gases, but holds the others fixed to values in the US Standard Atmosphere. The carbon dioxide profile is set to have a constant mixing ratio of 380 ppmv, and the contributions from chlorofluorocarbons (CFCs) are not included in the model. The fastaeri model was constructed using output from the line-by-line radiative transfer model (LBLRTM) version 11.3, which includes the water vapor continuum model MT_CKD v2 (Clough et al. 2005). The fastaeri model has been used extensively in previous analyses of water vapor and temperature from the AERI (e.g., Smith et al. 1999).

Optimally, the formulation of Eq. 1 should guarantee the minimization of a quadratic cost function between $\mathbf{x}_a$ and $\mathbf{x}_i$, and also between $\mathbf{y}$ and $\mathbf{y}_i$, when the difference between $\mathbf{x}_{i+1}$ and $\mathbf{x}_i$ goes towards zero. The iteration procedure is terminated after an optimal number of iterations ($i$=$op$) when IPT has converged to a sensible point; i.e., when the change in $\mathbf{x}_i$ is small. Here a quadratic cost function is applied to determine whether the retrieved $\mathbf{F}(\mathbf{x}_{op})$ is adequately close to the $\mathbf{F}(\mathbf{x}_{i-1})$ of the prior iteration. It is important to note that the solution $\mathbf{x}_{op}$ must be interpreted as the most probable solution of a Gaussian distributed probability density function, whose covariance can be written as:

$$\mathbf{S}_{op} = \left(\mathbf{K}_i^T \mathbf{S}_e^{-1} \mathbf{K}_i + \mathbf{S}_a^{-1}\right)^{-1}. \qquad (2)$$

The diagonal elements of this matrix give an estimate of the mean quadratic error of $\mathbf{x}_{op}$, whereas the off-diagonal elements yield information on the correlation of retrieval errors between the different heights.

A further important measure for retrieval algorithm evaluation is the averaging kernel matrix $\mathbf{A}$ which states the sensitivity of the retrieved to the true state (= $\partial \mathbf{x}_{op}/\partial \mathbf{x}$). In the case of Gaussian statistics, $\mathbf{A}$ can be written as

$$\mathbf{A} = \mathbf{S}_{op} \cdot \left(\mathbf{K}_i^T \mathbf{S}_e^{-1} \mathbf{K}_i\right). \qquad (3)$$

The diagonal values of $\mathbf{A}$ are frequently used as a measure of vertical resolution (Rodgers, 2000) whereas the trace of $\mathbf{A}$ states the independent number of levels which can be retrieved from a given measurement.

### 3.2. A priori information

In this study our goal is to show the potential of a combined AERI + HATPRO observation system for temperature and humidity retrieval. For this reason we do not use any other a priori information besides a long-term radiosonde climatology. Löhnert et al. (2007) have shown how the microwave profiler retrievals can be enhanced by including additional in-situ measurements such as close-by radiosonde ascents. However this paper's main goal is to assess the accuracy of the temperature and humidity retrievals from microwave and infrared observations using only the observations from the radiometers themselves. To evaluate the information content from the two instruments relative to each other, we utilize data from two climatically different stations.

The first station considered is Payerne, Switzerland, which represents a typical central European climate, located at 46.49 N and 6.97 E at 492 m above sea level. Here the a priori profiles $\mathbf{x}_a$ were calculated as seasonal means using 9446 radiosonde ascents over a time period from 1992 to 2006. All radiosondes were subject to a sophisticated quality control procedure (Noerenberg et al. 2008) to guarantee the use of only physically realistic ascents. The second station considered is Darwin, Australia, which represents a humid tropical climate, located at 12.42 N and 130.89 E at 30 m above sea level. Here 2218 radiosonde ascents over a time period from 1992 to 2005 passed the quality control procedure and thus were used to determine the a priori profiles. The covariance matrices $\mathbf{S}_a$ were calculated four times for each station (i.e., as a function of season), with the variances of T and $\rho_v$ at each vertical level on the diagonal and the covariances between the different levels in the off-diagonal components. Note that the covariances between T and $\rho_v$ have also been considered.

### 3.3. Se Matrix

For this simulation study the error covariance matrix $\mathbf{S}_e$ contained only non-zero elements on the diagonal components and the off-diagonal components were set to zero, which assumes that the measurement uncertainties are wavelength independent. This matrix is used to describe the expected measurement accuracy of the HATPRO and AERI instruments. For the HATPRO simulations, the error numbers were set to the square values of the noise levels listed in Tab. 1. These error estimates include both typical radiometric noise and calibration drifts as well as random uncertainties in the absorption model. In the generation of the virtual observations dataset, these values are randomly added to the forward model calculations to create simulated measurements.

The random noise in the AERI observations is determined from the imaginary component of the calibrated radiance (Knuteson et al. 2004b), and thus any scene-dependence of the noise level is automatically captured. For this sensitivity study, we utilized the average noise level of a normal-sampling AERI system in clear sky cases (Knuteson et al. 2004b). This translates into 1-sigma uncertainties of bands A1 – A4 given in Tab. 1. The square of these values was used along the diagonal of the $\mathbf{S}_e$ matrix, and zeros were utilized on the off-diagonal. The zeros on the off-diagonal components used in both the HATPRO and AERI $\mathbf{S}_e$ matrices imply that there is no correlation of error between the channels, an assumption frequently made for simplicity and lack of knowledge.

## 4. Retrieval Evaluation

For this analysis, HATPRO brightness temperatures and AERI radiances have been simulated from the pressure, temperature and humidity profiles of a subset of “clear sky” (CS) radiosonde ascents spanning all seasons; this amounted to 620 cases at Payerne an 643 cases at Darwin. The CS classification was based on a threshold in relative humidity; radiosondes were classified as CS if they did not show a relative humidity of more than 95% throughout the profile. The difference in climatology of these two sites is shown in the distributions of surface temperature and IWV (Fig. 2). The Payerne site shows a much cooler and broader (282.1 ± 7.5 K) distribution of surface temperature in comparison to the Darwin site (300.6 ±

2.2 K) indicating fairly hot and constant low-level temperatures at the latter site. However, Darwin shows a higher standard variation in IWV (12.5 kg $m^{-2}$) with values peaking around 70 kg $m^{-2}$ and a mean value of 40.2 kg $m^{-2}$ in comparison to 14.9 ± 7.3 kg $m^{-2}$ at the Payerne site. These two significantly different sites were chosen for retrieval evaluation in order to test the sensitivities of the MW and IR retrievals under a wide range of conditions.

In this section we apply the above described retrieval method to six different setups of the measurement vector **y**. The first four setups encompass two microwave and two infrared retrieval configurations (see Tab. 1). The microwave zenith-only (MZ) setup applies only zenith-looking observations from all the HATPRO channels (Bands M1 and M2), whereas the microwave zenith plus elevation retrieval (ME) additionally uses the 4 most optically thick channels of Band M2 at five further elevation angles (42., 30., 10.2, 19.2, and 5.4 degrees above the horizon). The standard AERI retrieval setup (AE) applies measurements between 538 and 588 $cm^{-1}$ (Band A1) and 1250 and 1350 $cm^{-1}$ (Band A3) for water vapor profile information and additionally one side of the 15 μm $CO_2$ band from 674 to 713 $cm^{-1}$ (Band A3) for temperature profiling. The second AERI (AE4) retrieval setup uses the standard AERI setup plus the channels from 2223 to 2260 $cm^{-1}$ (Band A4). The remaining two retrieval configurations then constitute the physical combinations of MZ & AE (MZAE) and MZ & AE4 (MZAE4) to allow joint retrievals to be evaluated.

### 4.1. Retrieval example

As an example, the two spectra in Fig. 1, which represent typical dry and moist cases, were used as input into the MW and IR retrieval algorithms (Fig. 3). In the moist summer case, both the MZ and the AE retrieval show very similar results in matching the almost dry-adiabatic lapse rate in the lower troposphere. The spectral information content in both microwave and infrared data is too low to resolve the lifted inversion around 4 km, as the weighting functions for these ground-based sensors become quite broad in the middle-to-upper troposphere. This is why we have restricted our analysis to heights below 5 km in the following. The temperature retrieval for the drier winter case clearly shows that the AE retrieval is able reproduce the strong lifted inversion more accurately than the MZ retrieval, which shows clear “smoothing” effects. This also holds true for both summer and winter time humidity profile retrievals. The AE retrieval shows potential to retrieve distinct features of the humidity profiles, such as the fairly constant $\rho_v$ values in the BL and the following abrupt decrease with height in the winter case, as well as the humidity increase around 2 km in the summer case.

Additionally, the diagonal components of $\mathbf{S}_{op}$ have been evaluated for retrieval error characterization (Fig. 4). As expected from Fig. 3, the AE retrieval for T and $\rho_v$ has a smaller retrieval error than MZ, both in the winter and summer cases. Note that for the winter case, the $\boldsymbol{\rho}_v$ accuracy of AE is almost a factor four better than of MZ. For these two examples, the differences in accuracy between MZ and AE are more pronounced for the wintertime case. In order to test the sensitivity towards the instrument random noise assumption, the HATPRO and AERI noise levels have been multiplied by 0.5 and 2 and the retrieval was then re-applied (Fig. 4). For the shown cases, the changes in MZ retrieval accuracy (8-18 %) are much less sensitive to the instrument random noise level than the changes in AE retrieval accuracy (40-100%). Especially in case of the MZ humidity retrievals, the instrument noise level has hardly any influence on the retrieval accuracy above 1.2 km (winter) and 2.5 km (summer), respectively. This suggests that the MW measurements add no significant amount of information to retrieval accuracy above these heights. However, the retrieval will still perform more accurately than the assumption of the seasonal priori profile due to the level correlation contained in $\mathbf{S}_a$. The much higher sensitivity of AE to the assumed instrumental noise reflects the fact that there is generally more information contained in the AERI compared to the HATPRO measurements. On the one hand, if the error noise assumptions for the AERI (Tab. 1) are too conservative and or are significantly reduced by principal component analysis (section 3.3), AE retrievals may be much more accurate than assumed. On the other hand, if the AERI errors are larger than expected, MZ may even outperform AE – especially in high humidity cases above the lower BL.

**4.2. Statistical retrieval evaluation**

In this section we apply the retrieval technique to the six different configurations of the measurement vector **y** (Tab. 2). Figures 5 – 8 show the derived accuracies from the retrieval simulations as a function of height above ground. Each of these figures only shows an analysis of those cases where all of the shown methods converged simultaneously. Due to this, the number of cases shown in each figure may vary, but is noted in each figure caption.

**i) Payerne**

The performance of the different single instrument retrievals (Fig. 5) show similar temperature RMSE accuracies in the lowest 500 m for ME, AE and AE4 ranging from 0.2 to 0.5 K. These low error values are very suitable for lower BL profiling and underlines that HATPRO in elevation scanning mode is able to perform similarly to the AERI in this range. At higher altitudes the ME accuracies more closely resemble those of MZ, which performs poorest throughout the lowest 5 km. MZ accuracies range from 0.5 K in the lower boundary layer to ~2 K at 5 km. Both AE and AE4 accuracies, on the contrary, remain below 1 K up to 4 km height. AE and AE4 accuracies are very similar showing that the use of the shoulder of the $CO_2$ absorption band between 675-713 $cm^{-1}$ is sufficient for a highly accurate temperature retrieval. Furthermore, this study has not accounted for the possible solar scattering contribution to the 4 µm signal that may result from an aerosol loaded sky, which would further impact the accuracy of the retrieval in the AE4 configuration. The accuracies of the humidity retrieval in the BL show significant differences between HATPRO and AERI. The AE accuracies are as low as 0.25 g $m^{-3}$ in the lower BL, slowly increasing to 0.6 g $m^{-3}$ at 2 km, whereas the MZ retrieval shows constant values around 0.75 g $m^{-3}$ in the same height range. Thus, as also indicated in the example profiles in Fig. 3, the AERI retrievals show the ability to resolve more vertical humidity structure than the HATPRO retrievals. However both AERI and HATPRO retrievals are still significantly more accurate than the mean seasonal climatology (which is indicated by the a priori profiles as dotted lines). For both temperature and humidity retrievals, bias errors are rather small compared to the RMSE. Of all humidity retrievals, MZ and ME exhibit the largest bias errors in the range of -0.15 g $m^{-3}$ in the lower 2.5 km and +0.15 g $m^{-3}$ in the upper 2.5 km, whereas the biases from AE and AE4 retrievals are insignificant. The bias of the a priori data is a result of regarding only a sub-sample of the original data from which the mean seasonal profiles were derived (i.e. the subset of cases that converged for all four retrieval methods). Figure 5b nicely shows that this "seasonal bias" is corrected for by all retrievals, however certain artefacts, such as the curvature between 3 and 4 km (Fig. 5b) are maintained. This is a result of the statistical correlation between each of the levels, which is prescribed in the $\mathbf{S}_a$ matrix.

The combination of both MZ and AE (MZAE) or MZ and AE4 (MZAE4) into one physical retrieval scheme shows no significant improvement in the retrieved temperature and humidity profiles compared to the AE retrieval alone in the Payerne dataset (Fig. 6). The behavior of the combined retrievals – both from the RMSE and bias error point of view – is very similar to that of AE. This clearly demonstrates that no significant additional information is added from the microwave profiler measurement to the spectral infrared measurements. This conclusion, however, is only strictly valid for an atmosphere containing no clouds and no significant amount of aerosol.

In the current retrieval configuration, the computation of the Jacobian matrix $\mathbf{K}_i$ requires a perturbation of 43 temperature and humidity values at each iteration step. Mainly due to the computing time for the forward calculations with the fastaeri model, this requires a significant amount of time for an AE profile to converge (order of 180 s on a standard Linux PC). Since future applications of this retrieval technique will include the retrieval of clouds and aerosol (and thus the inclusion of even more time consuming scattering calculations), it is of high desire to significantly reduce this calculation time without losing too much accuracy. In order to achieve this goal, Empirical Orthogonal Functions (EOF) have been separately derived for the temperature and humidity profile. Analysis of the EOF data reduction using the objective algorithm by Turner et al. (2006) showed that both temperature and humidity profiles at Payerne can be sufficiently described by 10 to 15 EOFs. Retrieving temperature and humidity profiles in EOF space for AE and subsequently transforming back into state space shows hardly any accuracy losses in terms of temperature (Fig. 7a-b). An exception may be the height range 800 to 1200 m where frequent BL topping inversions occur. The RMSE accuracy of humidity (Fig 7c) is also only slightly reduced in the lower 2 km – maximum RMSE increases are on the order of 0.1 g $m^{-3}$. Humidity bias error characteristics are not affected (Fig 7d). The advantage of the EOF decomposition is that computation time for a successful retrieval is reduced by a factor of 3-4.

**ii) Darwin**

In the much warmer and moister tropical climate, retrieval behavior (Fig. 8) does differ significantly to the central European climate (Fig. 5). RMSE values for all temperature retrievals in the lowest 500 m are lower at the Darwin site due to the less pronounced diurnal cycle in the tropics. Here, the lapse rate is frequently close to adiabatic, whereas typical night-time inversions and day time adiabatic lapse rates in central Europe result in a higher temperature variability of the BL. Specifically this increases the RMSE values of the MZ retrieval at the mid-latitude site, because it has the least information content concerning temperature and thus only limited ability in retrieving temperature inversions. Generally fewer inversions occur in the tropical climate, which are more difficult to capture with any retrieval algorithm. Above 1 km height, the addition of the microwave observations or the 4 µm observations to the AE retrieval results in a slight accuracy improvement of ~0.1 K. However, above 3 km, all RMSE curves slowly evolve towards the a priori RMSE curve indicating no benefit to retrieval at these heights.

In case of the humidity RMSE values at the tropical site, AE is only superior to MZ up to a height of ~ 1 km. Above this height, the large amounts of water vapor in the tropics result in a more opaque atmosphere for the AERI measurements, so that the vertical resolution at higher altitudes diminishes. However, the microwave channels are still much more transparent. As a consequence the MZAE combination shows the best RMSE results throughout the profile. Generally the RMSE humidity accuracies are poorer for the Darwin site than for the Payerne site, however the absolute values and also the variability are higher at Darwin. At both sites the improvements with respect to the a priori climatology are then similar, namely in the range between 0.5 and 0.8 g $m^{-3}$ within the height range up to 2 km. The a priori bias of both temperature and humidity for the chosen tropical sub-sets are higher than in the central European case. In case of temperature, as for the Payerne site, MZ shows the highest sensitivity to bias error, whereas the AERI retrievals are less sensitive and can compensate for the a priori bias in the lowest 2 km. Above this level the bias error of all retrievals follow the curvature of the a priori bias, with an overall reduction of bias error. In case of the humidity retrieval, the a priori bias of the data subset is too large to be entirely compensated by any retrieval, although the retrievals including the AERI observations show less a priori bias sensitivity in the lowest 1.5 km. This result clearly shows that an a priori bias of this magnitude should be avoided. A possible solution to this problem would be to scale the a priori profile of humidity with a realistic and independent IWV value, e.g. obtainable from a close-by radiosonde measurement or a GPS measurement.

The main results discussed above are presented in an overview in Tab. 2. Here the RMSE have been averaged over the 0 – 5 km altitude range to show the benefits and drawbacks of each evaluated retrieval setup. This table underlines the high value of AERI vs. HATPRO observations in clear sky conditions for temperature and humidity profiling - especially in moderately humid climates.

### 4.3. Degrees of freedom

An objective way to analyze the information content of the different retrievals is to evaluate the distribution of the number of degrees of freedom of the each single retrieval (Eq. 3), i.e. the number of independent levels of temperature or humidity that can be determined. For temperature, the distributions of degrees of freedom of MZ and AE do not overlap; neither for the Payerne, nor for the Darwin site retrieval simulations (Figs. 9a and 9c). This clearly demonstrates that AE provides more information on the temperature profile than MZ – on average 5.6 as opposed to 2.4 independent layers. Fig. 9a also illustrates that the inclusion of the elevation scanning mode in the HATPRO measurements can double the amount of independently retrieved levels, but as seen from Fig. 5 this improvement is mostly limited to the lowest 500 m. As expected, ME and MZ do not differ with respect to the humidity retrievals since no additional information about the humidity profile has been added. For the

Darwin site simulations, in comparison to Payerne, the average number of independent levels is reduced for AE (from 6.3 to 4.2) and increased for MZ (from 1.6 to 2.7). As already discussed in section 4.2, the increasing opacity at the Band M1 microwave channels leads to a slightly improved height resolution, whereas the AERI measurements in Bands A1 and A3 are becoming more opaque and thus resolve the height profile in a less accurate way in the moist tropical environment.

## 5. Conclusions and Outlook

We have presented simulation results from two independent ground-based remote sensing instruments, a standard microwave profiler (HATPRO) and an infrared spectrometer (AERI), for lower-tropospheric profiling of temperature and humidity in clear sky conditions. In order to compare both methods objectively, all measurements have been simulated realistically and consistently, and the same optimal estimation retrieval framework was applied to both using the same a priori information. Generally the infrared retrievals "outperform" the microwave retrievals concerning RMSE and bias error. The AERI retrievals show high potential, especially for retrieving humidity in the BL, where accuracies are better than 0.5 g $m^{-3}$ for a central European climate. In the lowest 500 m the retrieval accuracies for temperature from elevation scanning microwave measurements and spectral infrared measurements are very similar and are on the order of 0.2 – 0.6 K. Distinct differences occur between a tropical and central European climate, where the inclusion of microwave measurements to the spectral infrared measurements within a unified physical retrieval scheme results in a slight improvement due to the higher opacity of the very moist atmosphere in the tropics.

The conclusions drawn above are only valid in 'pristine' clear sky situations. Aerosols can significantly enhance the observed downwelling infrared radiance signal, depending on the aerosol size distribution, optical depth, and composition (e.g., Turner 2008). The simulations presented above have not included aerosol, which will pose an issue when applying the retrieval schemes to real measurements. In order for a clear sky retrieval to be successful, an objective classification scheme must be available to rule out the presence of clouds and aerosol, or the radiance contribution from the aerosol and/or cloud layer must be incorporated into the retrieval (either as a priori information or retrieved simultaneously). Note that even very small amounts of column integrated liquid water content (~1 g $m^{-2}$) can lead to non-negligible signals in an AERI measurement (Turner 2007). If, before the application of a clear-sky retrieval, it cannot be ruled out that clouds or aerosols (especially hydroscopic aerosols leading to cloud formation) are present, a microwave-only retrieval may turn out to be more accurate, because passive microwave measurements are insensitive to aerosol and optically thin clouds.

In this sense, the present study is to be regarded as a starting point for the development towards a joint thermodynamic and cloud / aerosol retrieval scheme including microwave and infrared measurements. The simultaneous use of microwave and AERI observations to retrieve cloud properties only has already been demonstrated by Turner (2007) and Turner and Eloranta (2008). We are currently setting up and testing a sophisticated retrieval scheme for temperature, humidity, cloud phase discrimination, cloud optical depth and cloud effective radius from simultaneous AERI and HATPRO measurements. In contrast to the results shown here, we expect significant improvements in the retrieved atmospheric state by the AERI/HATPRO combination due to the fact that clouds are semi-transparent in the microwave region. In case of an optically thick cloud in the infrared, which occurs when the liquid water path is above approximately 60 g $m^{-2}$, the AERI measurements will yield accurate information on temperature and humidity profiles below the cloud and the cloud base temperature, as well as, to a certain extent, cloud optical depth, whereas the microwave measurements will give information on temperature and humidity throughout and above the cloud, in addition to the total liquid water content. In the case of an optically thin cloud, the

AERI will provide information on cloud effective radius and optical depth and the atmospheric state profiles below the cloud, whereas again the microwave radiometer will provide a reliable source on temperature and humidity profile throughout the troposphere.

**Acknowledgements**

This work has been supported in part by the U.S. Department of Energy, Office of Science, Office of Biological and Environmental Research, Environmental Sciences division as part of the Atmospheric Radiation Measurement (ARM) program under grant DE-FG02-06ER64167. Additionally the authors would like to thank Dr. Robert Knuteson for his valuable comments and suggestions for improvement of the manuscript.

**References**

Cady-Pereira, K.E., M.W. Shephard, D.D. Turner, E.J. Mlawer, S.A. Clough, and T.J. Wagner, 2008: Improved total column precipitable water vapor from Vaisala RS90 and RS92 radiosonde humidity sensors. *J. Atmos. Oceanic Technol.*, **25**, 873-883, doi:10.1175/2007JTECHA1027.1.

Clough, S.A., M.W. Shephard, E.J. Mlawer, J.S. Delamere, M.J. Iacono, K. Cady-Pereira, S. Boukabara, and P.D. Brown, 2005: Atmospheric radiative transfer modeling: a summary of the AER codes, Short communication. *J. Quant. Spectrosc. Radiative Transfer*, **91**, 233-244.

Crewell, S., and U. Löhnert, 2007: Accuracy of boundary layer temperature profiles retrieved with multi-frequency, multi-angle microwave radiometry. *IEEE Trans. Geosci. Remote Sensing*, in press.

Eyre, J.R, and H.M. Woolf, 1988: Transmittance of atmospheric gases in the microwave region: A fast model. *Appl. Opt.*, 27, 3244-3249

Feltz, W. F.; Smith, W. L.; Howell, H. B.; Knuteson, R. O.; Woolf, H. and Revercomb, H. E., 2003: Near-continuous profiling of temperature, moisture, and atmospheric stability using the Atmospheric Emitted Radiance Interferometer (AERI). *J. Appl. Meteor.*, **42**, 857-875.

Feltz, W.F., W.L. Smith, R.O. Knuteson, H.E. Revercomb, and H.B. Howell, 1998: Meteorological applications of temperature and water vapor retrievals from the ground-based Atmospheric Emitted Radiance Interferometer (AERI). *J. Appl. Meteor.*, **37**, 857-875.

Knuteson, R.O., and coauthors, 2004a: Atmospheric Emitted Radiance Interferometer. Part I: Instrument design. *J. Atmos. Oceanic Technol*., **21**, 1763-1776.

Knuteson, R.O., and coauthors, 2004b: Atmospheric Emitted Radiance Interferometer. Part II: Instrument performance. *J. Atmos. Oceanic Technol*., **21**, 1777-1789.

Löhnert, U., S. Crewell, O. Krasnov, E. O'Connor, H. Russchenberg, 2008: Advances in Continuously Profiling the Thermodynamic State of the Boundary Layer: Integration of Measurements and Methods, *J. Atmos. Oceanic Technol. – in press*

Löhnert, U., E. van Meijgaard, H. Klein Baltink, S. Groß, and R. Boers, 2007: Accuracy assessment of an integrated profiling technique for operationally deriving profiles of temperature, humidity and cloud liquid water. *J. Geophys. Res.*, **112**, D04205, doi:10.1029/2006JD007379

Löhnert, U., S. Crewell, and C. Simmer, 2004: An integrated approach towards retrieving physically consistent profiles of temperature, humidity, and cloud liquid water. *J. Appl. Meteor.*, **43**, 1295-1307

Nörenberg, D., S. Crewell, U. Löhnert, T. Rose, 2008: Development of Ground Equipment for Atmospheric Propagation Conditions Assessment from 10 up to 90 GHz Frequency Bands (ATPROP) - ESA CONTRACT 19839/06/NL/GLC, Final Report, available through Institute for Geophysics and Meteorology, University of Cologne, Germany – *in press*

Rodgers, C. D., 2000: *Inverse methods for atmospheric sounding: Theory and practice*. World Scientific, 238 pp.

Rose, T., S. Crewell, U. Löhnert, and C. Simmer, 2005: A network suitable microwave radiometer for operational monitoring of the cloudy atmosphere. *Atmos. Res.*, Special issue: CLIWA-NET: Observation and Modelling of Liquid Water Clouds, **75**, 183-200, doi:10.1016/j.atmosres.2004.12.005.

Rosenkranz, P. W., 1998: Water vapour microwave continuum absorption: A comparison of measurements and models. *Radio Sci.*, **33**, 919–928.

Smith, W.L., W.F. Feltz, R.O. Knuteson, H.E. Revercomb, H.M. Woolf, and H.B. Howell, 1999: The retrieval of planetary boundary layer structure using ground-based infrared spectral radiance measurements. *J. Atmos. Oceanic Technol*., **16**, 323-333.

Turner, D.D., and E.W. Eloranta, 2008: Validating mixed-phase cloud optical depth rerieved from infrared observations with high spectral resolution lidar. *IEEE Geosci. Remote Sens. Lett.*, **5**, 285-288, doi:10.1109/LGRS.2008.915940.

Turner, D.D., 2007: Improved ground-based liquid water path retrievals using a combined infrared and microwave approach. *J. Geophys. Res.*, **112**, D15204, doi:10.1029/2007JD008530.

Turner, D.D., 2008: Ground-based retrievals of optical depth, effective radius, and composition of airborne mineral dust above the Sahel. *J. Geophys. Res.*, submitted.

Turner, D.D., R.O. Knuteson, H.E. Revercomb, C. Lo, and R.G. Dedecker, 2006: Noise reduction of Atmospheric Emitted Radiance Interferometer (AERI) observations using principal component analysis. *J. Atmos. Oceanic Technol.*, **23**, 1223-1238.

Turner, D.D., B.M. Lesht, S.A. Clough, J.C. Liljegren, H.E. Revercomb, and D.C. Tobin, 2003: Dry bias and variability in Vaisala radiosondes: The ARM experience. *J. Atmos. Oceanic Technol.*, **20**, 117-132.

**Figure Captions**

**Fig. 1**: Areas (grey-shaded) of the microwave (a) and infrared (b, c) spectra used for temperature and humidity profiling in this study. The light grey and black lines depict the spectra during a humid summer day at Payerne (IWV ~30 kg $m^{-2}$) and during a typical winter day with low amounts of water vapour (~8 kg $m^{-2}$), respectively. The associated atmospheric profiles are shown in Fig. 3.

**Fig. 2**: Distributions of surface temperature (a) and IWV (b) for the Payerne (N=620 cases) and Darwin (N=643 cases) sites during clear sky scenes.

**Fig. 3**: Profiles of temperature (a) and humidity (b) for a summer and winter case at Payerne. Shown are radiosonde measurements (grey), microwave zenith-only retrievals (MZ, dotted) and AERI retrievals without the 4 µm channel (AE, solid).

**Fig. 4**: Temperature and humidity accuracies (diagonal values of $\mathbf{S}_{op}$) for the wintertime and summertime cases shown in Fig. 3 as a function of assumed instrumental random noise. Dotted: noise as given in Tab. 1, solid: noise values multiplied by 0.5, dashed: noise values multiplied by 2. Black lines indicate results from AE retrieval, grey lines from MZ retrieval.

**Fig. 5**: Temperature (upper) and humidity (lower) root mean square (RMSE) (left) and bias (right) errors for the retrievals applied to the Payerne data set. Microwave zenith-only retrieval (MZ, solid), Microwave zenith + elevation angle retrieval (ME, dashed), AERI retrievals without the 4 µm channels (AE, dot-dashed), AERI retrievals with the 4 µm channels (AE4, dot-dot-dot-dashed). The error characteristics of the a priori profiles (mean seasonal climatology) are also shown (dotted). Note that the a priori RMSE of temperature is on the range of 4-5 K and thus not shown here. (N=304)

**Fig. 6**: Same as Fig. 5, only now that comparisons are carried for the Payerne station out for MZ (solid), AE (dashed), *combined microwave zenith and AERI retrievals without* the 4 µm channels (MZAE, dashed-dotted) and *combined microwave zenith and AERI retrievals with* the 4 µm channels (MZAE4, dot-dot-dot-dashed). (N=272)

**Fig. 7**: As Fig. 5, only now that comparisons are carried out for MZ (solid), AE (dashed), and *AERI retrievals derived with a EOF-decomposition* for temperature and humidity using 10 separate Eigenvectors for each variable (AE_EOF, dashed-dotted) (N=276).

**Fig. 8**: As Fig. 5, only now that comparisons are carried out for the *Darwin radiosonde site*; MZ (solid), AE (dashed), AE4 (dot-dashed) and MZAE (dot-dot-dot-dashed) (N=459).

**Fig. 9:** Histograms of the number of degrees of freedom for temperature (left) and humidity (right) retrievals at the Payerne (upper) and Darwin (lower) sites. The different shading indicates the MZ, (horizontal lines) retrieval, the ME (slant lines) retrieval and the AE (grey shaded) retrieval.

**Figures:**

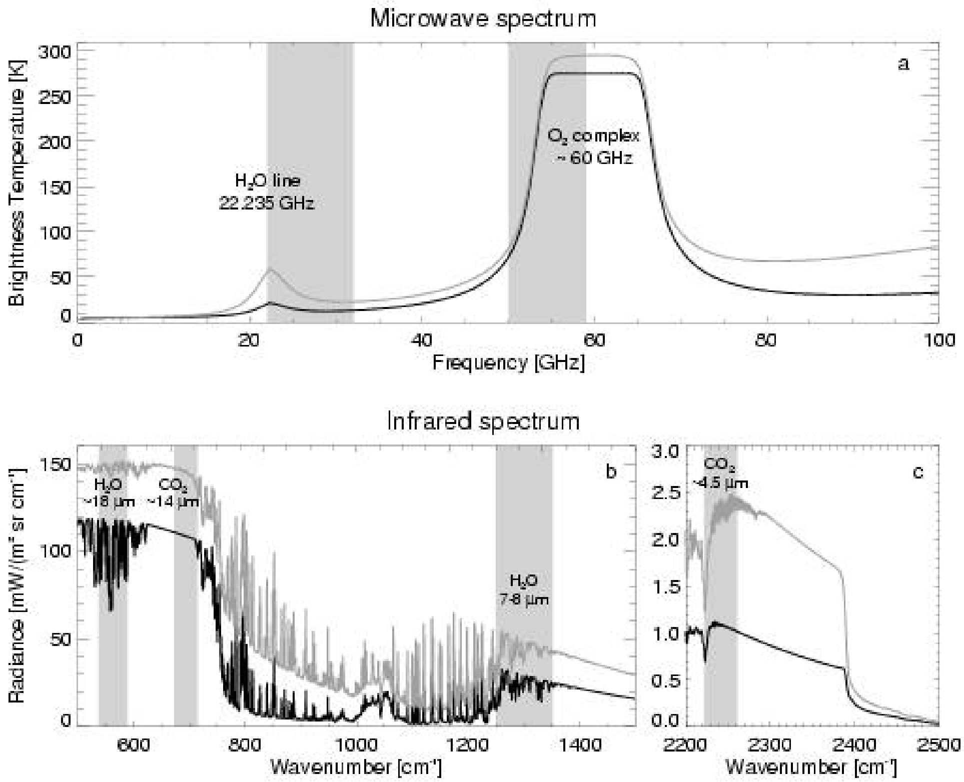


**Fig. 1**: Areas (grey-shaded) of the microwave (a) and infrared (b, c) spectra used for temperature and humidity profiling in this study. The light grey and black lines depict the spectra during a humid summer day at Payerne (IWV ~30 kg $m^{-2}$) and during a typical winter day with low amounts of water vapour (~8 kg $m^{-2}$), respectively. The associated atmospheric profiles are shown in Fig. 3.

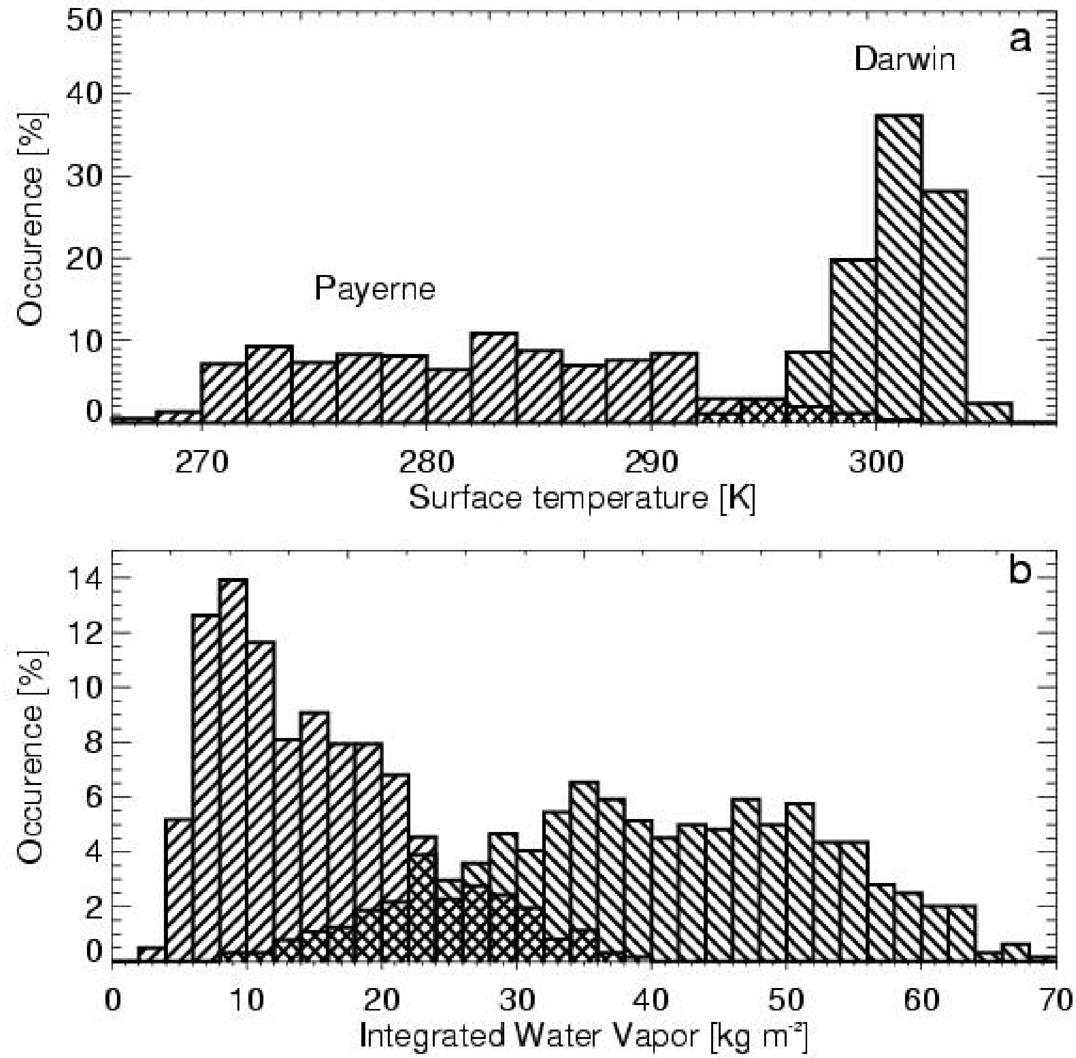


**Fig. 2**: Distributions of surface temperature (a) and IWV (b) for the Payerne (N=620 cases) and Darwin (N=643 cases) sites during clear sky scenes.

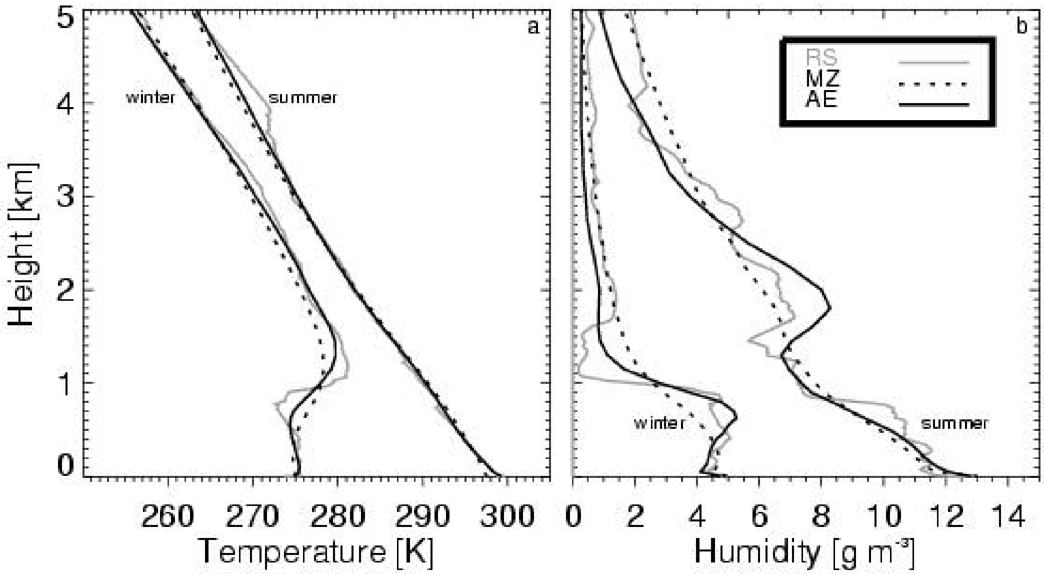


**Fig. 3**: Profiles of temperature (a) and humidity (b) for a summer and winter case at Payerne. Shown are radiosonde measurements (grey), microwave zenith-only retrievals (MZ, dotted) and AERI retrievals without the 4 µm channel (AE, solid).

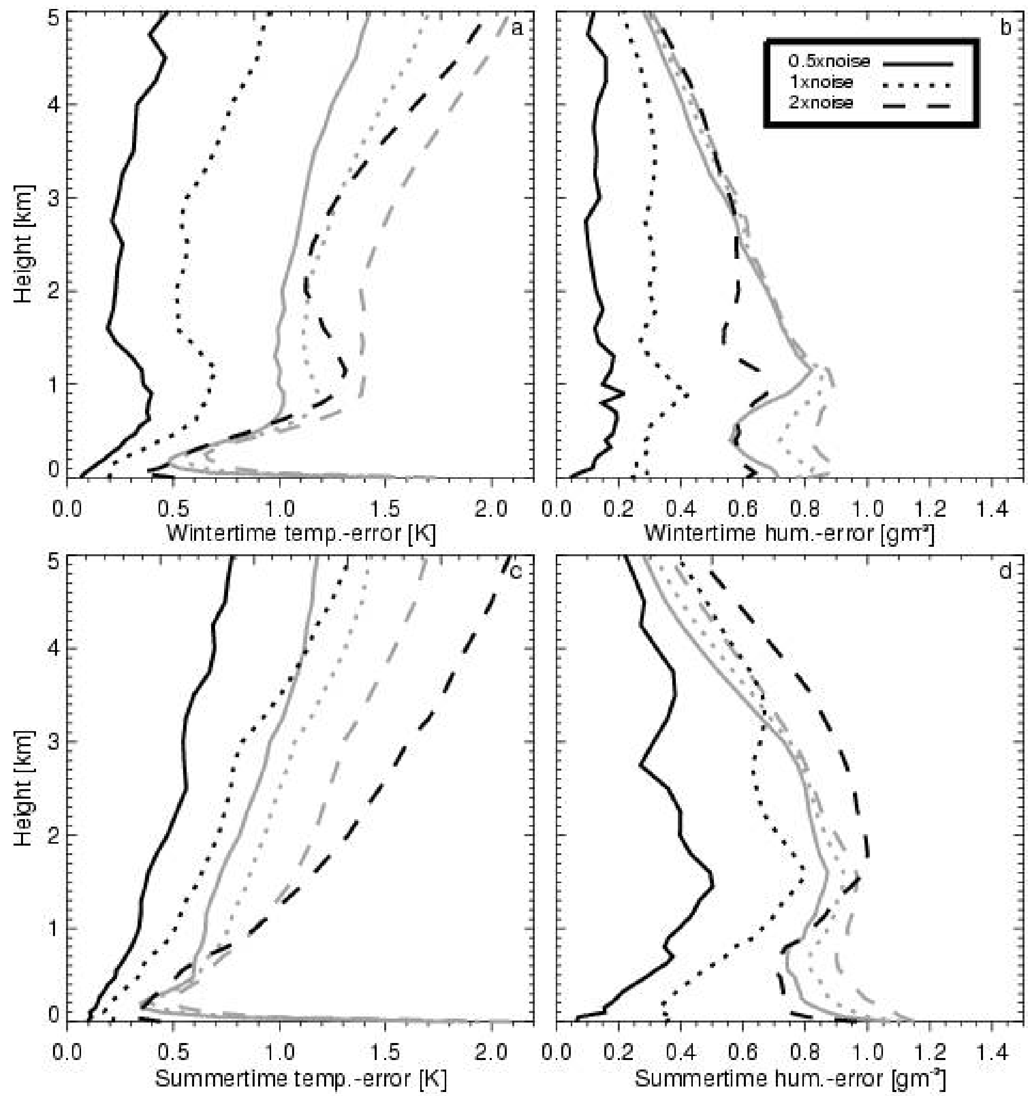


**Fig. 4**: Temperature and humidity accuracies (diagonal values of $\mathbf{S}_{op}$) for the wintertime and summertime cases shown in Fig. 3 as a function of assumed instrumental random noise. Dotted: noise as given in Tab. 1, solid: noise values multiplied by 0.5, dashed: noise values multiplied by 2. Black lines indicate results from AE retrieval, grey lines from MZ retrieval.

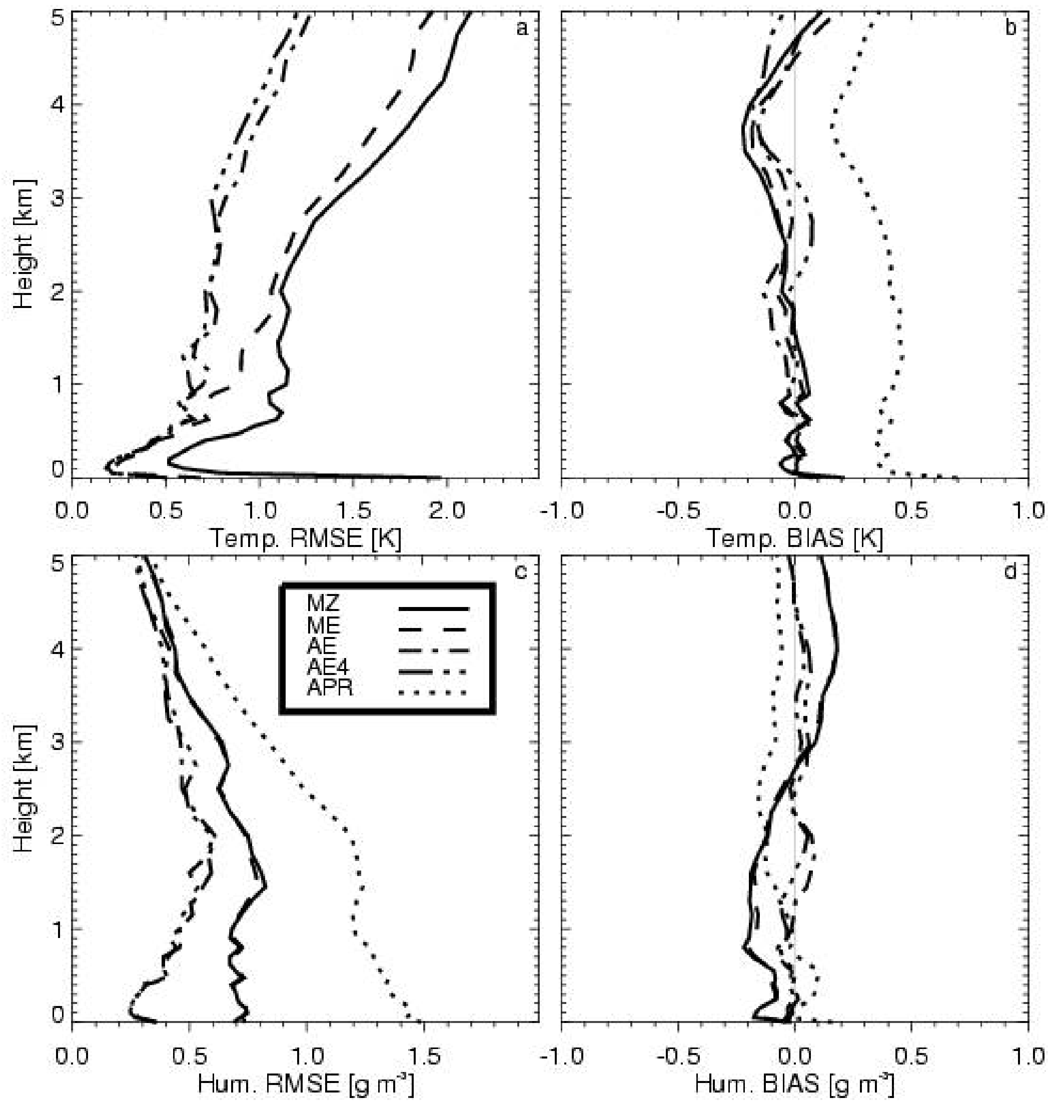


**Fig. 5**: Temperature (upper) and humidity (lower) root mean square (RMSE) (left) and bias (right) errors for the retrievals applied to the Payerne data set. Microwave zenith-only retrieval (MZ, solid), Microwave zenith + elevation angle retrieval (ME, dashed), AERI retrievals without the 4 µm channels (AE, dot-dashed), AERI retrievals with the 4 µm channels (AE4, dot-dot-dot-dashed). The error characteristics of the a priori profiles (mean seasonal climatology) are also shown (dotted). Note that the a priori RMSE of temperature is on the range of 4-5 K and thus not shown here (N=304).

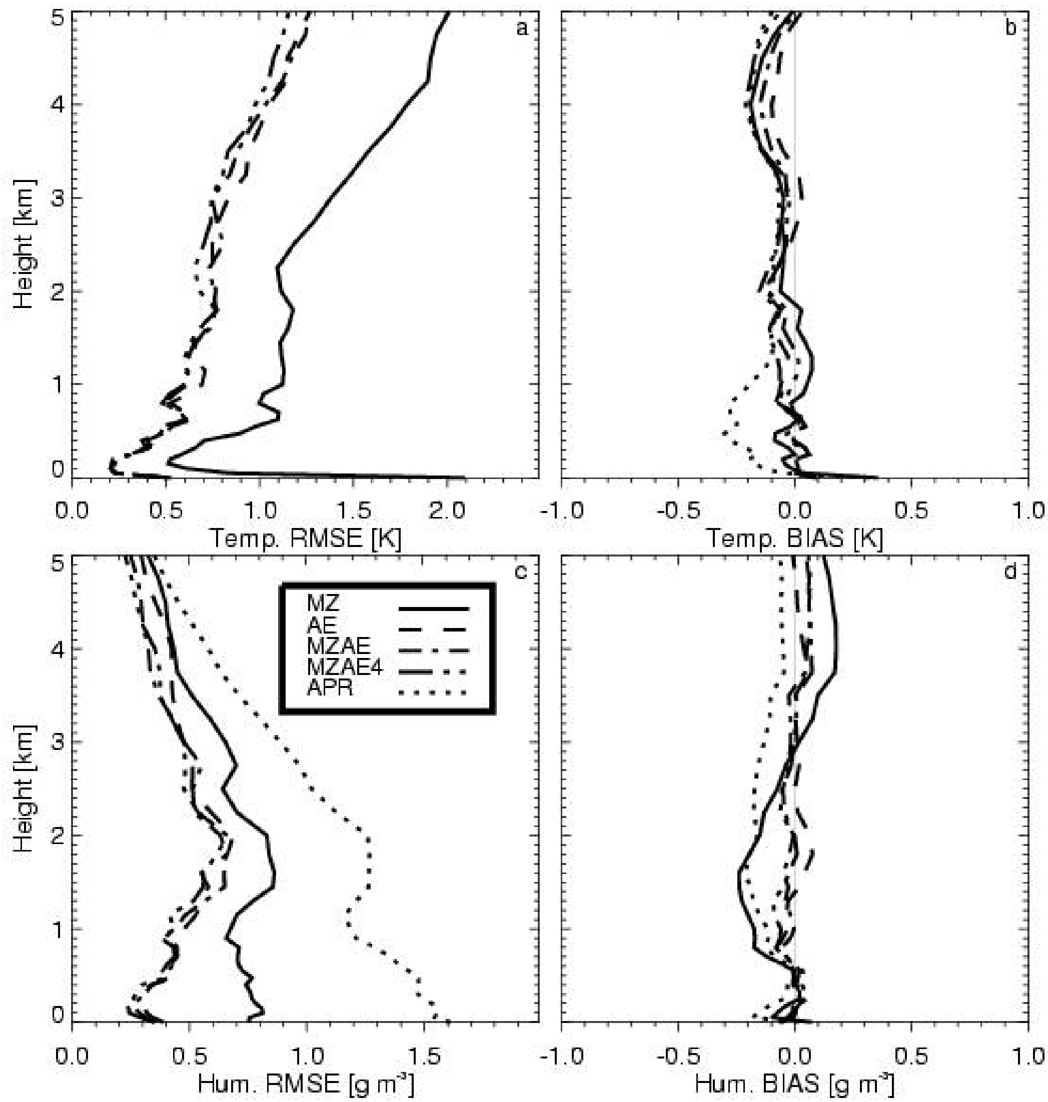


**Fig. 6**: Same as Fig. 5, only now that comparisons are carried for the Payerne station out for MZ (solid), AE (dashed), *combined microwave zenith and AERI retrievals without* the 4 µm channels (MZAE, dashed-dotted) and *combined microwave zenith and AERI retrievals with* the 4 µm channels (MZAE4, dot-dot-dot-dashed) (N=272).

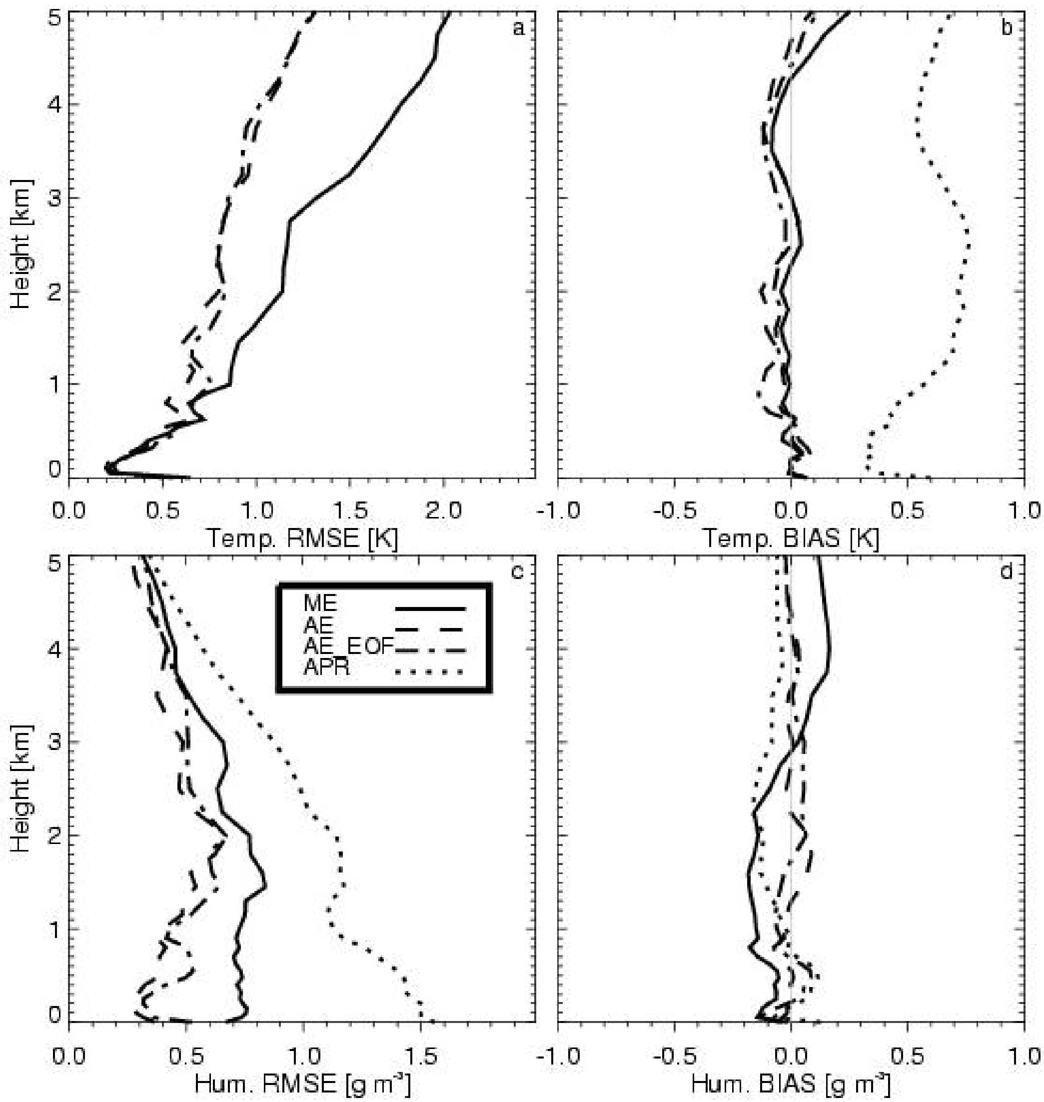


**Fig. 7**: As Fig. 5, only now that comparisons are carried out for MZ (solid), AE (dashed), and *AERI retrievals derived with a EOF-decomposition* for temperature and humidity using 10 separate Eigenvectors for each variable (AE_EOF, dashed-dotted) (N=276).

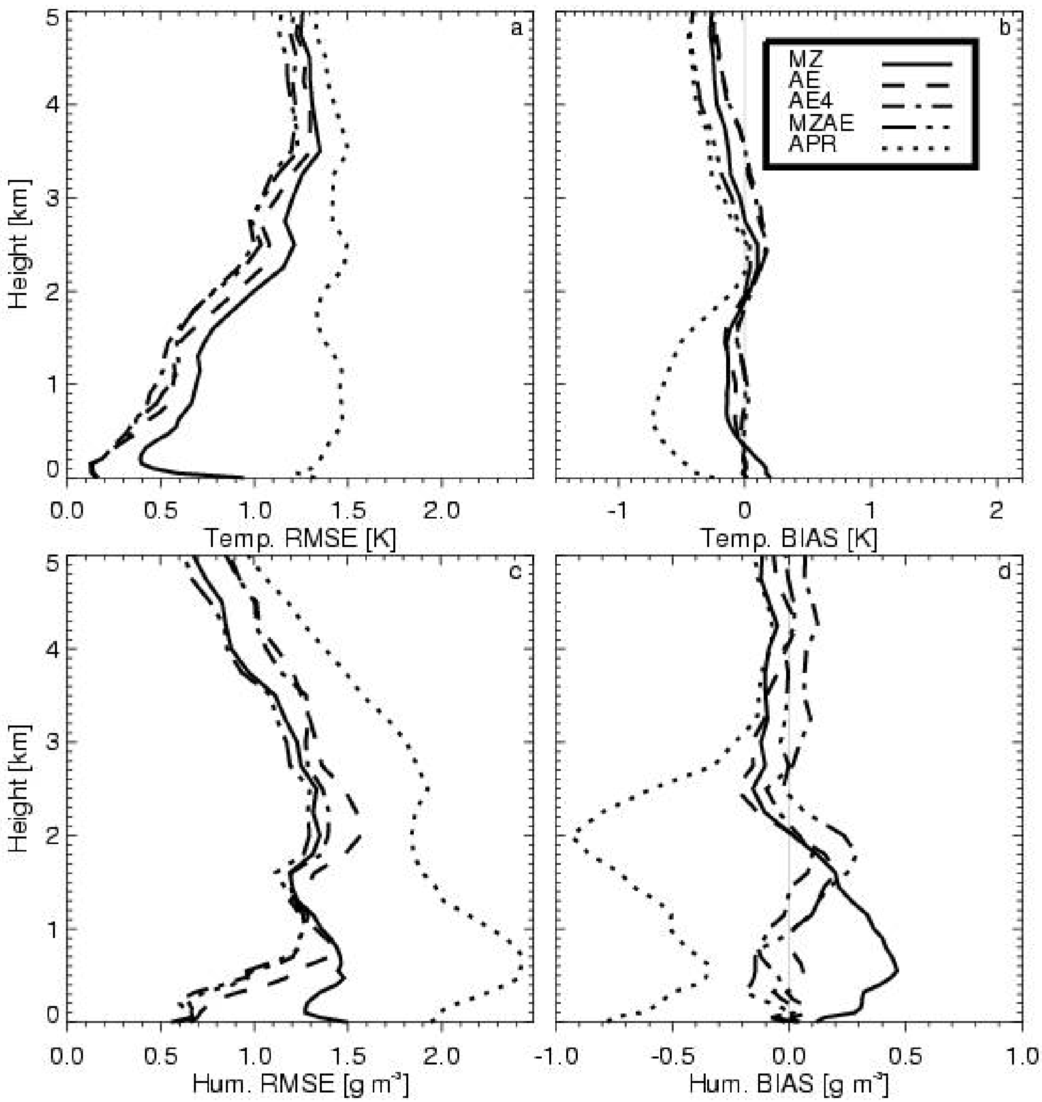


**Fig. 8**: As Fig. 5, only now that comparisons are carried out for the *Darwin radiosonde site*; MZ (solid), AE (dashed), AE4 (dot-dashed) and MZAE (dot-dot-dot-dashed) (N=459).

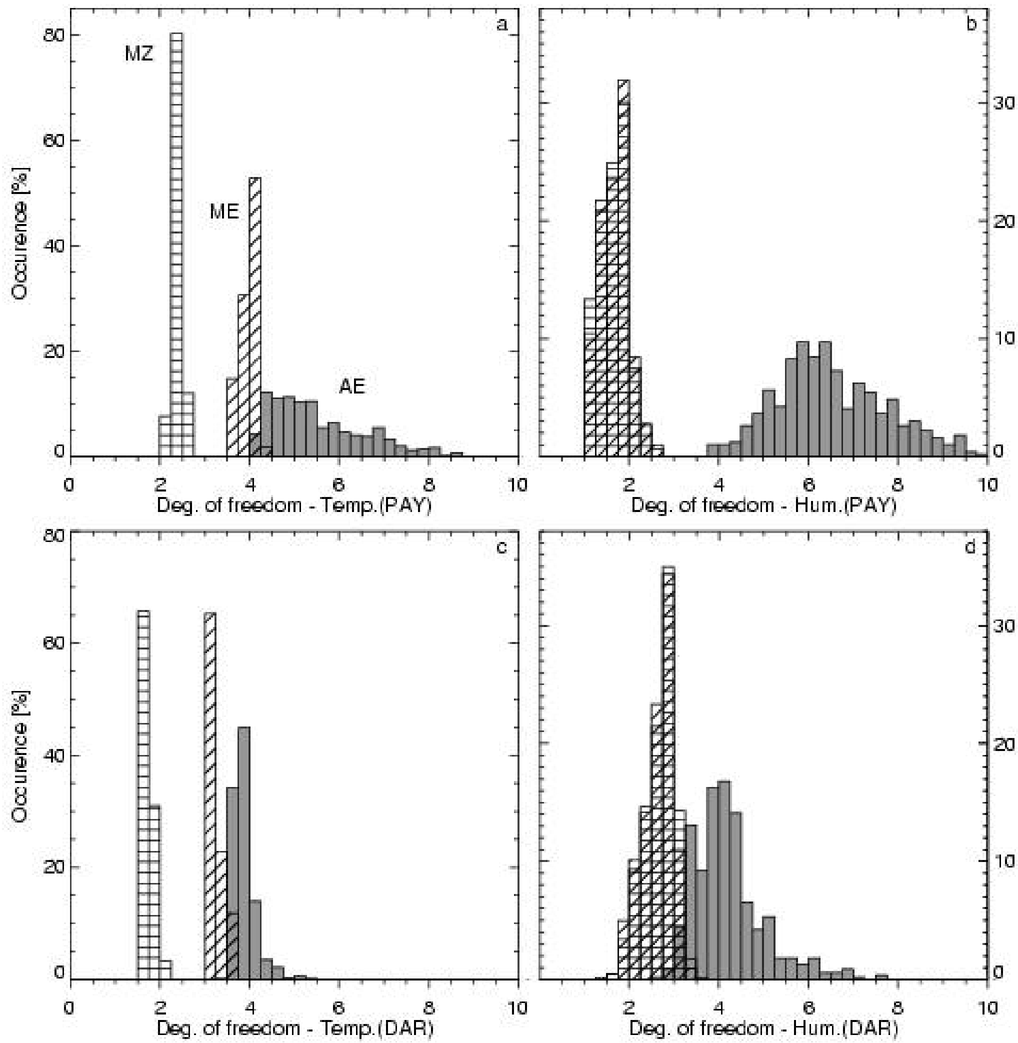


**Fig. 9**: Histograms of the number of degrees of freedom for temperature (left) and humidity (right) retrievals at the Payerne (upper) and Darwin (lower) sites. The different shading indicates the MZ, (horizontal lines) retrieval, the ME (slant lines) retrieval and the AE (grey shaded) retrieval.

**Tab. 1:** Description of microwave (M1, M2) and infrared (A1-A4) bands and the assumed instrumental noise used for the different retrieval setups.

| **Band M1**<br>center frequency (GHz) / Noise (K) | **Band M2**<br>center frequency (GHz) / Noise (K) | **Band A1**<br>range ($cm^{-1}$)<br>Number of Channels<br>Noise ($mW\ m^{-2}\ sr^{-1}\ cm$) | **Band A2**<br>range ($cm^{-1}$)<br>Number of Channels<br>Noise ($mW\ m^{-2}\ sr^{-1}\ cm$) | **Band A3**<br>range ($cm^{-1}$)<br>Number of Channels<br>Noise ($mW\ m^{-2}\ sr^{-1}\ cm$) | **Band A4**<br>range ($cm^{-1}$)<br>Number of Channels<br>Noise ($mW\ m^{-2}\ sr^{-1}\ cm$) |
|---|---|---|---|---|---|
| 22.24 / 0.4 | 51.26 / 0.5 | 538 – 588 | 675 – 713 | 1250 – 1350 | 2223 – 2260 |
| 23.04 / 0.4 | 52.28 / 0.5 | | | | |
| 23.84 / 0.4 | 53.86 / 0.5 | 104 | 79 | 208 | 77 |
| 25.44 / 0.4 | 54.94 / 0.2 | | | | |
| 26.24 / 0.4 | 56.66 / 0.2 | 1.8 | 0.30 | 0.25 | 0.011 |
| 27.84 / 0.4 | 57.30 / 0.2 | | | | |
| 31.40 / 0.4 | 58.00 / 0.2 | | | | |

**Tab. 2:** Description of different measurement configurations and their overall retrieval performance averaged over 0 - 5 km.

| Name | Measurements used | Temp. retrieval accuracy [K] – Mean RMSE 0-5km (Payerne / Darwin) | Hum. retrieval accuracy [$gm^{-3}$] – Mean RMSE 0-5km (Payerne / Darwin) |
|---|---|---|---|
| **MZ** | Bands M1, M2 | 1.22 / 0.86 | 0.66 / 1.23 |
| **ME** | Bands M1, M2, Elevation-scanning in Band M2 | 0.95 / 0.73 | 0.65 / 1.19 |
| **AE** | Bands A1, A2, A3 | 0.69 / 0.70 | 0.42 / 1.14 |
| **AE4** | Bands A1, A2, A3, A4 | 0.64 / 0.65 | 0.41 / 1.05 |
| **MZAE** | Bands M1, M2, A1, A2, A3 | 0.67 / 0.66 | 0.41 / 0.98 |
| **MZAE4** | Bands M1, M2, A1, A2, A3, A4 | 0.64 / - | 0.38 / - |